Commun. Theor. Phys. (Beijing, China) **37** (2002) pp 155–160
© International Academic Publishers
Vol. 37, No. 2, February 15, 2002

Moments and Mean First-Passage Time of Parabolic-Bistable Potential System Driven by Colored Noise*

LIANG Gui-Yun,[1] CAO Li,[1,3] KE Sheng-Zhi[1,3] and WU Da-Jin[2,3]

[1]State Key Laboratory of Laser Technology, Huazhong University of Science and Technology, Wuhan 430074, China

[2]CCAST (World Laboratory), P.O. Box 8730, Beijing 100080, China

[3]Department of Physics, Huazhong University of Science and Technology, Wuhan 430074, China

(Received April 27, 2001; Revised July 9, 2001)

Abstract *A parabolic-bistable potential system driven by colored noise is studied. The exact analytical expressions of the stationary probability distribution (SPD) and the moments of the system are derived. Furthermore, the mean first-passage time is calculated by the use of two approximate methods, respectively. It is found that (i) the double peaks of SPD are rubbed-down into a flat single peak with the increasing of noise intensity; (ii) a minimum occurs on the curve of the second-order moment of the system vs. noise intensity at the point $D_\Gamma = 0.025$; (iii) the results obtained by our approximate approach are in good agreement with the numerical calculations for either small or large correlation time τ, while the conventional steepest descent approximation leads to poor results.*

PACS numbers: 05.40.-a, 82.20.Mj, 02.50.-r, 02.60.-x
Key words: moments, mean first-passage time, colored noise, parabolic-bistable potential

1 Introduction

Recent studies show apparently that fluctuations play essential and active roles in many noise-induced phenomena such as phase lock in the laser,[1] escape rate in a bistable system,[2] noise-induced transport[1] and stochastic resonance.[3] As a typical and important example, the bistable system has been widely recognized and extensively investigated for many years. An electronic computer uses Boolean algebra to deal with calculation process and information deposition in which the basic elements 0 and 1 are actually carried out through controlling a bistable device. Moreover, in order to invent a photon computer, the design and manufacture of an optical bistable device are key technologies. It is very important to explore a bistable system driven by stochastic force. Firstly, a bistable system is a fundamental theoretical model for studying nonequilibrium phase transitions which contain many essential characteristics in nonlinear stochastic systems.[4] Secondly, a bistable device is technically based on the research for the statistical properties of a bistable model.

There are different types of bistable potentials. One important example is an absorbing optical bistable state which can be transformed into the form of particle movement in a potential field,[4] i.e., $\dot{x} = -U'_y(x)$, the potential function is $U_y(x) = yx - x^2/2 - C\ln(1+x^2)$. Considering a driving stochastic force $\Gamma(t)$, the equation is changed into Langevin equation $\dot{x} = -U'_y(x) + \Gamma(t)$, the bistable parameter $C > 4$. When the mode y of an input laser varies in the region of (y_-, y_+), $U_y(x)$ is a bistable potential field of mode x in the output laser, where $y_\pm = (C \pm \sqrt{C^2 - 4C} - 1)[1 + 2/(1 \pm \sqrt{1 - 4/C})]$. Another example is a quartic-bistable system driven by stochastic force $\Gamma(t)$, i.e., $\dot{x} = -U'(x) + \Gamma(t)$, where $U(x) = -\mu x^2/2 + x^4/4$, which is the most important model in nonlinear systems driven by noises.

Regarding the theoretical studies on the statistical properties in a quartic-bistable stochastic system, even if $\Gamma(t)$ is a Gaussian white noise (i.e., the process is Markovian), the exact analytical expressions of statistical properties have not yet been obtained so far.[4] Furthermore, if $\Gamma(t)$ is a colored noise, the process becomes non-Markovian. Much more efforts are limited to develop various approximate approaches to obtain approximate analytical expressions of the statistical properties.[4–8]

This paper is aimed to construct a bistable system driven by an Ornstein–Uhlenbeck (O–U) noise in order to get the exact analytical expression of stationary probability distribution (SPD). The non-Markovian bistable system is connected by three parabolic potentials, thus can be named as the parabolic-bistable potential system. It is found that the SPD of a single parabolic potential system driven by O–U noise can be resolved exactly, and that of the whole system can be obtained exactly through connecting the SPD of the three parabolic-bistable potential systems while the connection condition terms of SPD presented in this paper are used, which indeed play the same role as the boundary condition term at the limited boundary. Based on the exact SPD of the parabolic-bistable potential system, we obtain the accurate expression of nth moments of the system. Also, the mean first-passage time (MFPT) is calculated by numerical integration, steepest descent approximation and the new approximate method developed in this paper. Two approximate approaches are compared with the numerical calculations.

*The project supported by National Natural Science Foundation of China under Grant No. 19975020

2 The Parabolic-Bistable Potential Model and SPD

2.1 *The Parabolic-Bistable Potential Model*

Considering overdamped particles in a potential $U(x)$ as shown in Fig. 1, the stochastic dynamics is subject to the following Langevin equation

$$\dot{x} = -U'(x) + \varepsilon(t)\,, \tag{1}$$

where

$$U(x) = \begin{cases} U_1(x) = \dfrac{a}{2}(x+1)^2 + \dfrac{k}{2}\,, & x \le -\dfrac{1}{\sqrt{3}}\,, \\ U_2(x) = \dfrac{b}{2}x^2\,, & -\dfrac{1}{\sqrt{3}} < x < \dfrac{1}{\sqrt{3}}\,, \\ U_3(x) = \dfrac{a}{2}(x-1)^2 + \dfrac{k}{2}\,, & x \ge \dfrac{1}{\sqrt{3}}\,, \end{cases} \tag{2}$$

and $a > 0$, $b < 0$, $|b| < 1/\tau$, and $\varepsilon(t)$ represents O–U noise with zero mean and autocorrelation

$$\langle \varepsilon(t)\varepsilon(t')\rangle = \frac{D_\Gamma}{\tau}\exp\Big(-\frac{|t-t'|}{\tau}\Big), \tag{3}$$

where D_Γ is the noise intensity, τ is noise correlation time. Equation (1) is a one-dimensional non-Markovian process, which can be transformed into two-dimensional Markovian process

$$\dot{x} = -U'(x) + \varepsilon(t)\,, \tag{4}$$

$$\dot{\varepsilon}(t) = -\frac{1}{\tau}\varepsilon(t) + \frac{1}{\tau}\Gamma(t)\,, \tag{5}$$

where $\Gamma(t)$ is Gauss white noise with zero mean and

$$\langle \Gamma(t)\Gamma(t')\rangle = 2D_\Gamma\delta(t-t')\,. \tag{6}$$

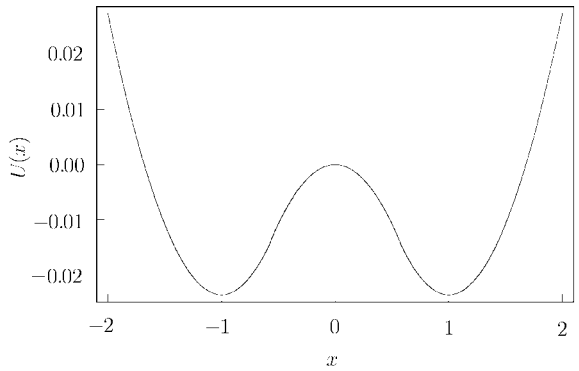

Fig. 1 The parabolic-bistable potential $U(x)$. The parameters are $\tau = 0.756$, $b = -0.0866025$, $k = -0.0425$ and $a = 0.102567$.

Because of the complexity of parabolic-bistable potential in Eq. (2), it is impossible to solve the Fokker–Planck equation corresponding to Eqs (2), (4) and (5) directly. However, we notice that the parabolic-bistable potential (2) can be divided into three regions. The SPD of x can be obtained exactly in each region. The SPD of x in the whole space can be obtained through connecting the three SPDs. The SPD in each region is derived in the following.

2.2 *The SPD in a Non-Markovian Parabolic Potential System*

Making a transform

$$y(t) = -U'(x) + \varepsilon(t)\,, \tag{7}$$

equations (4) and (5) become

$$\dot{x} = y\,, \tag{8}$$

$$\dot{y}(t) = \Big(-U''(x) - \frac{1}{\tau}\Big)y - \frac{1}{\tau}U'(x) + \frac{1}{\tau}\Gamma(t)\,. \tag{9}$$

Because the potentials $U_i(x)$ $(i = 1, 2, 3)$ in three regions are parabolic nonlinear of x (see Eq. (2)), $U''(x)$ is constant. Inserting $U_1(x)$, $U_2(x)$ and $U_3(x)$ in Eq. (2) into Eqs (8) and (9), respectively, we obtain

$$\dot{x}(t) = y\,, \tag{10}$$

$$\dot{y}(t) = -\Gamma_i\ y - \frac{1}{\tau}U_i'(x) + \frac{1}{\tau}\Gamma(t)\,, \tag{11}$$

where

$$\Gamma_1 = a + \frac{1}{\tau}\,, \qquad \Gamma_2 = b + \frac{1}{\tau}\,, \quad \Gamma_3 = a + \frac{1}{\tau}\,,$$

$$U_1'(x) = a(x+1)\,, \quad U_2'(x) = bx\,, \quad U_3'(x) = a(x-1)\,.$$

The combination of Eqs (10) and (11) is the special case of Kramers equation, the corresponding Fokker–Planck equation[4] is given by

$$\frac{\partial P(x,y,t)}{\partial t} = -\frac{\partial}{\partial x}[yP(x,y,t)]$$
$$-\frac{\partial}{\partial y}\Big[\Big(-\Gamma_i y - \frac{1}{\tau}U_i'(x)\Big)P(x,y,t)\Big] + \frac{D_\Gamma}{\tau^2}\frac{\partial^2}{\partial y^2}P(x,y,t).$$

Thus the joint stationary probability distribution $P(x,y)$ can be calculated exactly

$$P_i(x,y) = \varphi_i(x)\exp(-k_i y^2)\,, \tag{12}$$

where

$$\varphi_i(x) = N\exp\Big[2k_i\int_{-\infty}^{x}\frac{1}{\tau}(-U_i'(x'))\,\mathrm{d}x'\Big], \tag{13}$$

$$k_i = \frac{c_i\ \tau^2 + \tau}{2D_\Gamma}\,, \quad c_1 = c_3 = a\,, \quad c_2 = b\,, \tag{14}$$

so that we have

$$P_i(x) = \int_{-\infty}^{\infty}P_i(x,\varepsilon)\,\mathrm{d}\varepsilon = \int_{-\infty}^{\infty}P_i(x,y)\ \Big|\ \frac{\partial(x,y)}{\partial(x,\varepsilon)}\ \Big|\ \mathrm{d}\varepsilon\,.$$

By making use of Eqs (12) ∼ (14), we get

$$P_1(x) = N\sqrt{\frac{2\pi D_\Gamma}{a\tau^2+\tau}}\exp\Big[-\frac{a(a\tau+1)}{2D_\Gamma}(x+1)^2\Big], \qquad x \le -\frac{1}{\sqrt{3}}\,, \tag{15}$$

$$P_2(x) = N\sqrt{\frac{2\pi D_\Gamma}{b\tau^2+\tau}}\exp\Big[-\frac{b(b\tau+1)}{2D_\Gamma}x^2\Big], \qquad -\frac{1}{\sqrt{3}} < x < \frac{1}{\sqrt{3}}\,, \tag{16}$$

$$P_3(x) = N\sqrt{\frac{2\pi D_\Gamma}{a\tau^2+\tau}}\exp\Big[-\frac{a(a\tau+1)}{2D_\Gamma}(x-1)^2\Big], \qquad x \ge \frac{1}{\sqrt{3}}\,. \tag{17}$$

2.3 *The SPD in a Parabolic-Bistable Potential Model*

Now we construct the SPD, $P(x)$, of parabolic-bistable potential from $P_1(x), P_2(x)$ and $P_3(x)$. The physical conditions require that $P_i(x)$ and $P_i'(x)$ must be continuous at the boundary, i.e. $x = -1/\sqrt{3}$ and $x = 1/\sqrt{3}$. Because of the symmetry, only the continuous condition is given explicitly at the point $x = -1/\sqrt{3}$,

$$P_1\Big(x = -\frac{1}{\sqrt{3}}\Big) = P_2\Big(x = -\frac{1}{\sqrt{3}}\Big), \tag{18}$$

$$P_1'\Big(x = -\frac{1}{\sqrt{3}}\Big) = P_2'\Big(x = -\frac{1}{\sqrt{3}}\Big). \tag{19}$$

From Eqs (15) $\sim$ (19), we obtain

$$P(x) = \begin{cases} NH_1(x)\exp\Big[-\dfrac{\alpha\ (x+1)^2}{2D_\Gamma}\Big], & x \le -\dfrac{1}{\sqrt{3}}\,, \\ NH_2(x)\exp\Big[-\dfrac{\beta x^2}{2D_\Gamma}\Big], & -\dfrac{1}{\sqrt{3}} < x < \dfrac{1}{\sqrt{3}}\,, \\ NH_3(x)\exp\Big[-\dfrac{\alpha(x-1)^2}{2D_\Gamma}\Big], & x \ge \dfrac{1}{\sqrt{3}}\,, \end{cases} \tag{20}$$

where

$$\alpha = a(a\tau + 1)\,, \qquad \beta = b(b\tau + 1)\,,$$

$$H_1(x) = H_3(x) = \sqrt{\frac{a\tau+1}{b\tau+1}}\exp\Big(-\frac{\beta}{2\sqrt{3}D_\Gamma}\Big),$$

$$H_2(x) = \sqrt{\frac{2\pi D_\Gamma}{b\tau^2+\tau}}\,,$$

N is the normalization constant. From Eqs (18) and (19), we obtain equations which are subject to

$$(b\tau+1)b = (a\tau+1)a(1-\sqrt{3}\,)\,. \tag{21}$$

It is obvious that the value of τ should satisfy the condition governed by Eq. (21) when the values of a and b are given in the parabolic-bistable potential model, which implies that equation (20) is only valid for a unique τ derived from Eq. (21). In this case, equation (20) can be named as a "single colored" noise theory. In other word, τ is not adjustable as a steering parameter when a, b are chosen. However, considering the importance of bistable systems in stochastic dynamics, it is necessary to further discuss the statistical properties of the parabolic-bistable potential model which is rather different from either the absorbing optical bistable system or the quartic-bistable one. Figure 2 shows the statistical characteristics in the parabolic-bistable potential system. When the noise intensity D_Γ increases, the SPD expands wider, and the deviation between the two maximal heights and the single minimal one reduces. As D_Γ becomes larger, the two peaks fade out, and the structure of the SPD becomes a "single wide peak" which indicates the effects of the potential barrier valley vanish and the whole process is controlled by the noise. On the other hand, the structure of $P(x)$ is mainly dominated by the deterministic parabolic-bistable potential when the noise intensity D_Γ is small. The two peaks grow higher and narrower and finally become two δ pulses as D_Γ approaches to zero. Indeed, for $D_\Gamma \to 0$, the system transits from a stochastic process to a deterministic one.

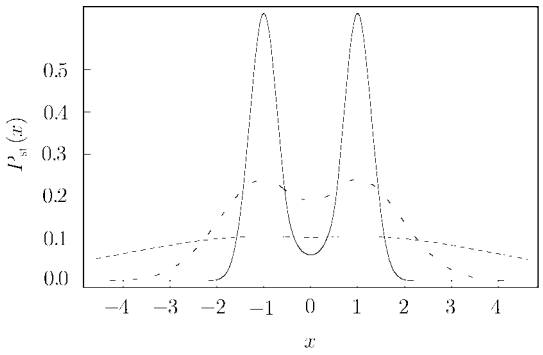

Fig. 2 The normalized SPD $P_{\rm st}(x)$. The parameters are $D_\Gamma = 1$ (dotted line), 0.1 (dashed line) and 0.01 (solid line), with $\tau = 0.756$, $b = -0.0866025$, and $a = 0.102567$.

3 Analytical Expressions of Moments

From Eq. (20), we can derive the nth order moment ($n = 1, 2, 3, \ldots$). Odd-number order moments $\langle x\rangle, \langle x^3\rangle, \ldots$ are equal to zero due to the symmetric relation. However, even-number higher-order moments cannot be obtained directly from the second-order moment because of the non-Gaussian distribution $P(x)$. Therefore, it is necessary to calculate $\langle x^n\rangle$ ($n = 2, 4, 6, \ldots$) besides the second-order moment. The second-order moment can be obtained easily,

$$\begin{aligned}\langle x^2\rangle = {} & \int_{-\infty}^{-1/\sqrt{3}} x^2 NH_1(x)\exp\Big[-\frac{\alpha(x+1)^2}{2D_\Gamma}\Big]\,\mathrm{d}x + \int_{-1/\sqrt{3}}^{1/\sqrt{3}} x^2 NH_2(x)\exp\Big[-\frac{\beta x^2}{2D_\Gamma}\Big]\,\mathrm{d}x \\ & \times \int_{1/\sqrt{3}}^{\infty} x^2 NH_3(x)\exp\Big[-\frac{\alpha(x+1)^2}{2D_\Gamma}\Big]\,\mathrm{d}x \\ = {} & 2NH_1(x)\Big\{\sqrt{\frac{\pi D_\Gamma}{2\alpha}}\Phi\Big[(1-\sqrt{3}\,)\sqrt{\frac{\alpha}{6D_\Gamma}}\Big]\Big(\frac{D_\Gamma}{\alpha}+1\Big) + \frac{D_\Gamma(\sqrt{3}+1)}{\sqrt{3}\alpha}\exp\Big[-\frac{\alpha(\sqrt{3}-1)^2}{6D_\Gamma}\Big]\Big\} \\ & + 2NH_2(x)\sum_{n=0}^{\infty}\Big(\frac{-\beta}{2D_\Gamma}\Big)^n\frac{1}{2n+3}\Big(\frac{1}{\sqrt{3}}\Big)^{2n+3}, \end{aligned} \tag{22}$$

where the error function is

$$\Phi(x) = \frac{2}{\sqrt{\pi}}\int_0^x \exp(-t^2)\,\mathrm{d}t\,.$$

$\langle x^n\rangle$ $(n=2,4,6,\ldots)$ can be obtained through integration

$$\begin{aligned}\langle x^n\rangle &= \int_{-\infty}^{-1/\sqrt{3}} x^n N H_1(x)\exp\Big[-\frac{\alpha(x+1)^2}{2D_\Gamma}\Big]\,\mathrm{d}x + \int_{-1/\sqrt{3}}^{1/\sqrt{3}} x^n N H_2(x)\exp\Big[-\frac{\beta x^2}{2D_\Gamma}\Big]\,\mathrm{d}x \\ &\quad\times\int_{1/\sqrt{3}}^{\infty} x^n N H_3(x)\exp\Big[-\frac{\alpha(x+1)^2}{2D_\Gamma}\Big]\,\mathrm{d}x \\ &= 2NH_1(x)\Big(\frac{\alpha}{D_\Gamma}\Big)^{-(n+1)/2}\Gamma(n+1)\exp\Big(-\frac{\alpha}{4D_\Gamma}\Big)D_{-(n+1)}\Big(-\sqrt{\frac{\alpha}{2D_\Gamma}}\,\Big) \\ &\quad-2NH_1(x)\sum_{k=0}^{\infty}\Big(-\frac{\alpha}{2D_\Gamma}\Big)^k\sum_{i=0}^{\infty}C_{2k}^i\frac{(-1)^i}{n+i+1}\Big(\frac{1}{\sqrt{3}}\Big)^{n+i+1}+2NH_2(x)\sum_{k=0}^{\infty}\Big(-\frac{\beta}{2D_\Gamma}\Big)^k\frac{1}{n+2k+1}\Big(\frac{1}{\sqrt{3}}\Big)^{n+2k+1},\end{aligned}\tag{23}$$

in which

$$\Gamma(n+1)=(n+1)!,\qquad D_{-(n+1)}\Big(-\sqrt{\frac{\alpha}{2D_\Gamma}}\,\Big)=\frac{\exp[-\alpha/(8D_\Gamma)]}{\Gamma(n+1)}\int_0^\infty\exp\Big(\sqrt{\frac{\alpha}{2D_\Gamma}}\,x-\frac{x^2}{2}\Big)x^n\,\mathrm{d}x\,.$$

For $n=2$, equation (23) returns to Eq. (22).

The second and fourth moments are depicted in Fig. 3. An interesting phenomenon is found that $\langle x^n\rangle$ exhibits a minimum with the monotonical increasing of noise intensity D_Γ. It is apparent from the point of view of mathematics. For $D_\Gamma\to\infty$, $H_2(x)\to\infty$; for $D_\Gamma\to 0$ and $\beta<0$, $H_1(x)\to\infty$ and $H_2(x)\to\infty$. Therefore, $\langle x^n\rangle$ must experience a minimum with the monotonical increasing of D_Γ. Figure 3 also shows that the minimum becomes smaller for higher-order moment.

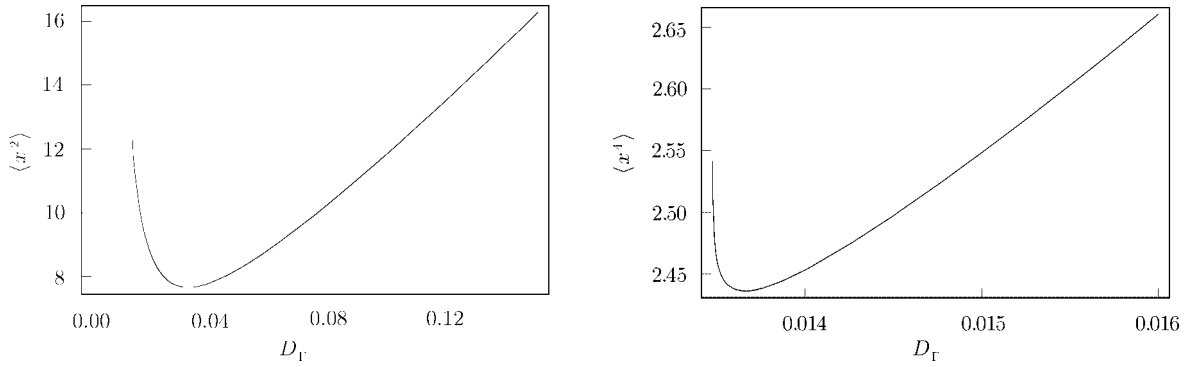

Fig. 3 The second-order moment $\langle x^2\rangle$ and quartic-order moment $\langle x^4\rangle$ vs. noise intensity D_Γ with parameters $\tau=0.756$, $b=-0.0866025$ and $a=0.102567$.

4 Mean First-Passage Time (MFPT)

When particles surmount a potential starting from $x=-1$ to $x=+1$, the MFPT is determined by[8]

$$T(D_\Gamma)=D_\Gamma^{-1}\int_{-1}^{1}H(x)\exp[\phi(x)/D_\Gamma]\,\mathrm{d}x\int_{-\infty}^{x}H(y)\exp[-\phi(y)/D_\Gamma]\,\mathrm{d}y\,.\tag{24}$$

Equation (24) is derived by two approximate procedures which are compared with direct numerical integrations, respectively.

4.1 *New Approximation*

$$\begin{aligned}T(D_\Gamma)&=D_\Gamma^{-1}\int_{-1}^{1}H(x)\exp[\phi(x)/D_\Gamma]\,\mathrm{d}x\int_{-\infty}^{x}H(y)\exp[-\phi(y)/D_\Gamma]\,\mathrm{d}y \\ &=D_\Gamma^{-1}\int_{-1}^{-1/\sqrt{3}}H_1(x)\exp[\phi_1(x)/D_\Gamma]\,\mathrm{d}x\int_{-\infty}^{x_1}H_1(y)\exp[-\phi_1(y)/D_\Gamma]\,\mathrm{d}y \\ &\quad+D_\Gamma^{-1}\int_{-1/\sqrt{3}}^{1/\sqrt{3}}H_2(x)\exp[\phi_2(x)/D_\Gamma]\,\mathrm{d}x\int_{-\infty}^{-1/\sqrt{3}}H_1(y)\exp[-\phi_1(y)/D_\Gamma]\,\mathrm{d}y \\ &\quad+D_\Gamma^{-1}\int_{-1/\sqrt{3}}^{1/\sqrt{3}}H_2(x)\exp[\phi_2(x)/D_\Gamma]\,\mathrm{d}x\int_{-1/\sqrt{3}}^{x_2}H_2(y)\exp[-\phi_2(y)/D_\Gamma]\,\mathrm{d}y\end{aligned}$$

$$+ D_\Gamma^{-1}\int_{1/\sqrt{3}}^{1} H_1(x)\exp[\phi_3(x)/D_\Gamma]\,\mathrm{d}x\int_{-\infty}^{-1/\sqrt{3}} H_1(y)\exp[-\phi_1(y)/D_\Gamma]\,\mathrm{d}y$$
$$+ D_\Gamma^{-1}\int_{1/\sqrt{3}}^{1} H_1(x)\exp[\phi_3(x)/D_\Gamma]\,\mathrm{d}x\int_{-1/\sqrt{3}}^{1/\sqrt{3}} H_2(y)\exp[-\phi_2(y)/D_\Gamma]\,\mathrm{d}y$$
$$+ D_\Gamma^{-1}\int_{1/\sqrt{3}}^{1} H_1(x)\exp[\phi_3(x)/D_\Gamma]\,\mathrm{d}x\int_{1/\sqrt{3}}^{x_3} H_1(y)\exp[-\phi_3(y)/D_\Gamma]\,\mathrm{d}y\,, \tag{25}$$

where $\phi_1(x)=\alpha(x+1)^2/2$, $\phi_2(x)=\beta x^2/2$, $\phi_3(x)=\alpha(x-1)^2/2$ and $\alpha>0$, $\beta<0$.

Performing dual integration on the right-hand side of Eq. (25), we get

$$\begin{aligned}T(D_\Gamma)=D_\Gamma^{-1}\Big\{&\int_{-1}^{-1/\sqrt{3}}\mathrm{d}x_1 H_1(x_1)\exp[\phi_1(x_1)/D_\Gamma]H_1(x_1)\sqrt{\frac{\pi D_\Gamma}{2\alpha}}\Big[1+\Phi\Big(\sqrt{\frac{\alpha}{2D_\Gamma}}(x_1+1)\Big)\Big]\\
&+2H_1H_2\int_0^{1/\sqrt{3}}\mathrm{d}x_2\exp[\phi_2(x_2)/D_\Gamma]\sqrt{\frac{\pi D_\Gamma}{2\alpha}}\Big[1+\Phi\Big(\sqrt{\frac{\alpha}{2D_\Gamma}}\Big(1-\frac{1}{\sqrt{3}}\Big)\Big)\Big]\\
&+2H_2^2\int_0^{1/\sqrt{3}}\mathrm{d}x_2\exp[\phi_2(x_2)/D_\Gamma]\int_{-1/\sqrt{3}}^{x_2}\exp[-\phi_2(y)/D_\Gamma]\,\mathrm{d}y\\
&+H_1^2\int_{1/\sqrt{3}}^{1}\mathrm{d}x_3\exp[\phi_2(x_3)/D_\Gamma]\sqrt{\frac{\pi D_\Gamma}{2\alpha}}\Big[1+\Phi\Big(\sqrt{\frac{\alpha}{2D_\Gamma}}\Big(1-\frac{1}{\sqrt{3}}\Big)\Big)\Big]\\
&+2H_1H_2\int_{1/\sqrt{3}}^{1}\mathrm{d}x_3\exp[\phi_2(x_3)/D_\Gamma]\int_0^{1/\sqrt{3}}\mathrm{d}y\exp\Big[-\frac{\beta y^2}{2D_\Gamma}\Big]\\
&+H_1^2\int_{1/\sqrt{3}}^{1}\mathrm{d}x_3\exp[\phi_2(x_3)/D_\Gamma]\sqrt{\frac{\pi D_\Gamma}{2\alpha}}\Big[\Phi\Big(\sqrt{\frac{\alpha}{2D_\Gamma}}\Big(1-\frac{1}{\sqrt{3}}\Big)\Big)+\Phi\Big(\sqrt{\frac{\alpha}{2D_\Gamma}}(x_3-1)\Big)\Big]\Big\}.\end{aligned}$$

Transforming variables $x_1, x_3 \to x$, we have

$$\begin{aligned}T(D_\Gamma)=D_\Gamma^{-1}\Big\{&H_1^2\sqrt{\frac{\pi D_\Gamma}{2\alpha}}\int_{-1}^{-1/\sqrt{3}}\mathrm{d}x\exp\Big[\frac{\phi_1(x)}{D_\Gamma}\Big]\sqrt{\frac{\pi D_\Gamma}{2\alpha}}\Big[1+\Phi\Big(\sqrt{\frac{\alpha}{2D_\Gamma}}\Big(1-\frac{1}{\sqrt{3}}\Big)\Big)\\
&+\frac{H_2}{H_1}\sqrt{\frac{2\alpha}{\pi D_\Gamma}}\int_0^{1/\sqrt{3}}\mathrm{d}y\exp\Big(-\frac{\beta y^2}{2D_\Gamma}\Big)\Big]+H_1H_2\sqrt{\frac{2\pi D_\Gamma}{-\beta}}\Phi\Big(\sqrt{\frac{-\beta}{6D_\Gamma}}\Big)\sqrt{\frac{\pi D_\Gamma}{2\alpha}}\\
&\times\Big[1+\Phi\Big(\sqrt{\frac{\alpha}{2D_\Gamma}}\Big(1-\frac{1}{\sqrt{3}}\Big)\Big)\Big]+H_2^2\int_{-1/\sqrt{3}}^{1/\sqrt{3}}\mathrm{d}x_2\exp\Big(\frac{\beta x_2^2}{2D_\Gamma}\Big)\int_{-1/\sqrt{3}}^{x_2}\mathrm{d}y\exp\Big(-\frac{\beta y^2}{2D_\Gamma}\Big)\Big\}.\end{aligned}\tag{26}$$

Since the first and the second integrated functions are even functions on the right-hand side of Eq. (26), and the second integration has symmetric integration region, we take the upper limit $x_2=0$ in the second integration, which leads the first integration to be available. Thus the approximate expression is obtained

$$\begin{aligned}T(D_\Gamma)=D_\Gamma^{-1}\Big\{&H_1^2\sqrt{\frac{\pi D_\Gamma}{2\alpha}}\int_{-1}^{-1/\sqrt{3}}\mathrm{d}x\exp\Big[\frac{\phi_1(x)}{D_\Gamma}\Big]\sqrt{\frac{\pi D_\Gamma}{2\alpha}}\Big[1+\Phi\Big(\sqrt{\frac{\alpha}{2D_\Gamma}}\Big(1-\frac{1}{\sqrt{3}}\Big)\Big)\\
&+\frac{H_2}{H_1}\sqrt{\frac{2\alpha}{\pi D_\Gamma}}\int_0^{1/\sqrt{3}}\mathrm{d}y\exp\Big(-\frac{\beta y^2}{2D_\Gamma}\Big)\Big]+H_1H_2\sqrt{\frac{2\pi D_\Gamma}{-\beta}}\Phi\Big(\sqrt{\frac{-\beta}{6D_\Gamma}}\Big)\sqrt{\frac{\pi D_\Gamma}{2\alpha}}\\
&\times\Big[1+\Phi\Big(\sqrt{\frac{\alpha}{2D_\Gamma}}\Big(1-\frac{1}{\sqrt{3}}\Big)\Big)+\frac{H_2}{H_1}\sum_{n=0}^{\infty}\Big(\frac{-\beta}{2D_\Gamma}\Big)^n\frac{1}{2n+1}\Big(\frac{1}{\sqrt{3}}\Big)^{2n+1}\Big]\Big\}.\end{aligned}\tag{27}$$

It is seen that the deviation arises from the integration of the region $|x|\le 1/\sqrt{3}$. Due to $\beta<0$, the last term on the right-hand side of Eq. (26) can be considered as the formal integral

$$\int_{-1}^{1}\mathrm{d}x\exp(-x^2)\int_{-1}^{x}\mathrm{d}y\exp(y^2)\,. \tag{28}$$

The first integration in Eq. (28) is weighted by the second integration. The first integration is regarded as a sum,

$$\sum_{i=0}^{n}K_i\exp(-x_i^2)\Delta x_i\,,\quad (x_0<x_1<\cdots<x_n)\,,$$

and $x_0=-1$, $x_n=1$, where

$$K_i=\int_{-1}^{x_i}\mathrm{d}y\exp(y^2)\,.$$

Here we take K_i as a constant identically equal to the

value at $x_i = 0$, which enlarges the weighted-coefficient of the first integration in the region of $x_i < 0$, but reduces in the region of $x_i > 0$. Furthermore, the integrated function is just even, also the integration region is symmetric. Therefore, we take the upper limit $x = 0$ in the last term of the right-hand side of Eq. (26).

In Fact, for asymmetric integrated functions, excellent agreement will be obtained in comparison with the numerical result if the upper limit of the second integration is properly chosen. Generally, expression (28) can be regarded as an example searching for the gravity center of irregular object in which there only remains the uncertainty of the weighted-coefficient of first integration. If the weighted-coefficient is given, one can yield the gravity center of the object through variable transformation, also the upper limit can be determined. For instance, we extend expression (28) to a general form

$$\int_c^d f(x)\,\mathrm{d}x \int_c^x g(y)\,\mathrm{d}y\,. \tag{29}$$

Let $z = G(x) = \int_c^x g(y)\,\mathrm{d}y$, equation (29) becomes

$$\int_{c'}^{d'} z\frac{f[G^{-1}(x)]}{g(x)}\,\mathrm{d}x\,. \tag{30}$$

If the expression of $G(x)$ is given, the integration is feasible, and the position of the gravity center is known, i.e.,

$$K = \int_{c'}^{d'} z\frac{f[G^{-1}(z)]}{g(z)}\,\mathrm{d}z \Big/ \int_{c'}^{d'} \frac{f[G^{-1}(z)]}{g(z)}\,\mathrm{d}z\,.$$

Then the upper limit of integration can be determined by $z = G(x) = K$. Therefore, the new approximation is a universal approach.

4.2 *The Steepest Descent Approximation*

The MFPT is obtained through steepest descent approximation,[9]

$$T(D_\Gamma) = \frac{2\pi H_1 H_2}{\sqrt{|\beta|\alpha}} \exp\Big(\frac{\alpha(\sqrt{3}-1)^2 - \beta}{6D_\Gamma}\Big). \tag{31}$$

5 Discussion

In order to verify the reliability of the new approximation and the steepest descent approximation, equations (27) and (31) are compared with numerical integration from Eq. (24), respectively. Figure 4 shows clearly that for small correlation time ($\tau = 0.756$), the MFPT obtained by new approximation is of good agreement with the numerical calculation, which is much better than the one obtained from the steepest descent approximation. For large correlation time ($\tau = 20$), figure 5 shows an excellent agreement between the new approximate result and the numerical calculation. However, the steepest descent approximation performs worse result.

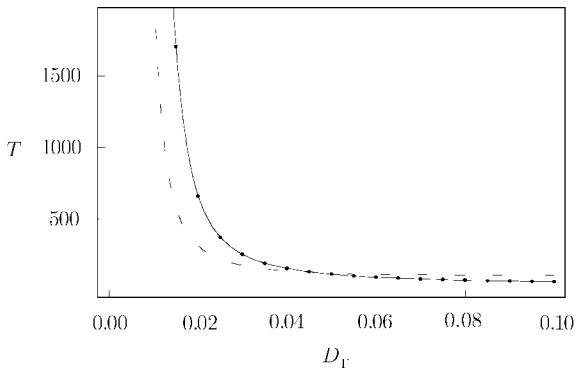

Fig. 4 The MFPT vs. noise intensity D_Γ. The solid line is numerical result (24); dotted line new approximation (27); dashed line the steepest descent approximation (31). The parameters are $\tau = 0.756$, $b = -0.0866025$ and $a = 0.102567$.

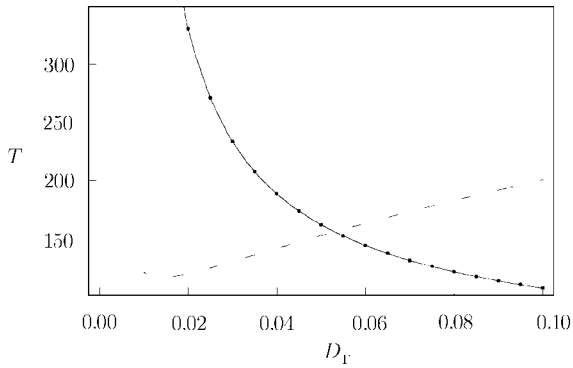

Fig. 5 The MFPT vs. noise intensity D_Γ. The solid line is numerical result (24); dotted line new approximation (27); dashed line the steepest descent approximation (31). The parameters are $\tau = 20$, $b = -0.0268468$ and $a = 0.013368$.

References

[1] L. CAO and D.J. WU, Phys. Lett. **A260** (1999) 126; L. CAO and D.J. WU, Phys. Lett. **A275** (2000) 223; L. CAO and D.J. WU, Phys. Rev. **E62** (2000) 7478.

[2] J.Y. YOU, L. CAO, D.J. WU and G.Y. LIANG, Chin. Phys. Lett. **18** (2001) 175.

[3] C.J. Tessone, H.S. Wio and P. Hänggi, Phys. Rev. **E62** (2000) 4623.

[4] G. HU, *Stochestic Forces and Nonlinear Systems*, Shanghai Scientific and Technological Education Publishing House (1994); G. Hu and H. Haken, Phys. Rev. **A41** (1991) 7078; G. Hu, Phys. Rev. **A43** (1991) 700; G. Hu and Z.H. Lu, Phys. Rev. **A44** (1991) 8027.

[5] M. Sancho, M. San Miguel, S.L. Kate and J.D. Gunton, Phys. Rev. **A26** (1982) 1589.

[6] P. Jung and P. Hänggi, J. Opt. Soc. Am. **B5** (1988) 979.

[7] F. Castro, H.S. Wio and G. Abranson, Phys. Rev. **E52** (1995) 159.

[8] A.J.R. Madureira and P. Hänggi, Phys. Rev. **E51** (1995) 3849; A.J.R. Madureira, P. Hänggi and H.S. Wio, Phys. Lett. **A271** (1996) 248.

[9] C.W. Gardiner, *Handbook of Stochastic Methods*, Springer-Verlag (1983).